Oil Shale, 2016, Vol. 33, No. 2, pp. 111–124
doi: 10.3176/oil.2016.2.02
ISSN 0208-189X

THE SIMULATION STUDY OF APPLICATION OF THE FG-DVC MODEL TO THE PYROLYSIS OF HUADIAN OIL SHALE OF CHINA AT DIFFERENT HEATING RATES

QING WANG, YIFAN WANG*, HONGXI ZHANG, XIANGCHENG XU, QIANKUN YANG, PING WANG

Engineering Research Centre of Oil Shale Comprehensive Utilization, Northeast Dianli University, Jilin 132012, China

Abstract. *In order to study the relationship between the chemical structure and pyrolysis products of oil shale, a series of experiments with Huadian oil shale of China were performed at various heating rates (10, 20 and 50 °C/min) by using Thermogravimetric Analysis-Fourier Transform Infrared Spectroscopy (TG-FTIR). The quantitative analysis of pyrolysis products, including CH_4, CO, CO_2, H_2O and shale oil, was carried out. The results showed the temperature at which the evolution rate of pyrolysis products reached a peak value. Also, the evolution rate was found to increase with increasing heating rate. For the abovementioned pyrolysis products, the values of kinetic parameters such as activation energy (E) and pre-exponent factor (A) were between 183 and 270 kJ·mol^{-1} and from 3.3 × 10^9 to 2.8 × 10^{13} s^{-1}, respectively. The Functional Group-Depolymerization Vaporization Crosslinking (FG-DVC) pyrolysis model based on the chemical structure of fuel was employed to simulate the evolution process of CH_4, CO, CO_2, H_2O and shale oil at three different heating rates: 10, 20 and 50 °C/min. The simulation results were in good agreement with TG-FTIR experimental data, indicating the applicability of the FG-DVC model to modelling the pyrolysis process of oil shale.*

Keywords: *oil shale pyrolysis, FG-DVC, kinetics, TG-FTIR.*

1. Introduction

Oil shale is classified as a high ash sapropel-type solid fossil fuel that contains combustible organic matter [1]. Similarities as well as differences exist between oil shale and coal, both are solid fossil fuels, yet their structure varies, with oil shale having more aliphatic chains [2]. In the thermal application of oil shale, pyrolysis as the initial stage of the conversion

* Corresponding author: e-mail *wef910621@126.com*

process that includes dry distillation and combustion is crucial, significantly influencing the subsequent stages of conversion [3]. Therefore, the creation of a pyrolysis model is of strategic importance to achieve an efficient use of oil shale with environmental and fiscal benefits.

Previous researches have reported various models which describe the pyrolysis process of coal, and can be divided into empirical and network models based on chemical structure [4]. The primary empirical models can be classified into single reaction models (single equation models), multiple parallel reaction models (distributed activation energy models) and competing overall reactions models [5–7]. In more recent years, with the development of modern laboratory techniques, including Thermogravimetric Analysis-Fourier Transform Infrared Spectroscopy (TG-FTIR), Pyrolysis-Flame Ionization Mass Spectrometry (Py-FIMS) and Carbon Nuclear Magnetic Resonance Spectroscopy (^{13}C-NMR), researchers have been able to investigate the pyrolysis mechanism based on the chemical structure of coal. Several network models such as the Functional Group-Depolymerization Vaporization Crosslinking (FG-DVC) [8–10], FLASHCHAIN [11] and chemical percolation and devolatilization (CPD) [12] models have been applied for this purpose. Although empirical models have played an important role in determining the yield and evolution rate of volatile compounds and describing the processes of combustion and gasification, the new tools facilitate to have a clearer picture of what is happening during the pyrolysis process in the composition and structure of samples since they are not related to their chemical structure. Therefore, network models provide a more effective manner of revealing the pyrolysis mechanism of fuel with respect to chemical structure.

In the literature, researchers have reported a number of oil shale pyrolysis models [13–16], yet all of which are still in the preliminary experimental verification stage and their universal applicability has to be determined. With the development and improvement of the contributions of Solomon et al. [8–10], the FG-DVC pyrolysis model has been widely implemented in the pyrolysis studies of coal as well as other fuels, such as biomass [17, 18] and coal water slurry [19]. The FG-DVC model has been employed to predict the yield of four lightweight gases and shale oil in the pyrolysis process of Chinese Gansu oil shale at a heating rate of 20 °C/min, which yielded promising results compared with TG-FTIR experimental data [20]. However, the applicability of this model to studying the pyrolysis of oil shales from the other regions of China or at other heating rates has not been confirmed yet. In this paper, in order to validate its applicability to oil shale pyrolysis, the FG-DVC model was employed to simulate the pyrolysis process of Huadian oil shale of China and predict the yield of pyrolysis products at heating rates of 10, 20 and 50 °C/min. Additionally, comparison between the experimental data obtained via TG-FTIR with those calculated by the FG-DVC model was made to verify its applicability to oil shale pyrolysis studies.

2. Experimental section

2.1. Sample preparation

In this paper, the oil shale samples were obtained from Huadian city, Jilin province, China. For experiments, the as-obtained samples were crushed in a jaw crusher and ground in a ball mill, then sieved to a size of 0–0.2 mm. Prior to pyrolysis, the experimental samples were dried in an oven at 110 °C for 2 h. Both the proximate and ultimate analyses of original oil shale samples were performed according to the Chinese National Standards. The proximate analysis was conducted according to the standard GB/T 30732-2014 Test method by instrumental procedures. The samples were analyzed for total carbon, oxygen, hydrogen and nitrogen contents by a chemical method according to the GB/T 476-2008 standard while the total sulfur content was determined by the standard GB/T 214-2007. Table 1 displays the data on proximate and ultimate analysis of oil shale samples.

Table 1. Proximate and ultimate analysis of oil shale samples

Proximate analysis, wt%				$Q_{net,ar}$, $kJ \cdot kg^{-1}$	Ultimate analysis, wt% (dry basis)				
M	C	A	FC		C	H	O	N	S
6.52	31.53	56.36	5.59	12271.2	18.25	4.03	13.28	0.58	0.98

Note: $_{ar}$ – as received

2.2. Instrumentation

TGA measurements were performed by a Mettler-Toledo thermogravimetric analyzer TGA/DSC1 with a nitrogen purge gas flow of 50 $ml \cdot min^{-1}$. The sample mass was placed in an open cylindrical alumina crucible (70 μLL). FTIR measurements were performed by a Thermo Electron Fourier transform infrared spectrometer Nicolet iS10 coupled to TGA equipped with a 20 cm optical path length infrared gas cell. The gas cell was equipped with a Cryogenic Mercury Cadmium Telluride (MCT) detector cooled with liquid nitrogen. The spectral range of the FTIR spectrometer was set to be 4000–400 cm^{-1} with a resolution and sensitivity of 4 cm^{-1} and 1.5, respectively. The TGA/DSC1 thermogravimetric analyzer system (METTLER-TOLEDO, Switzerland) was coupled with a Nicolet iS10 FTIR spectrometer (Thermo Electron, USA) through a heated stainless steel transfer line (1 m in length and 3.175 mm in internal diameter) with a temperature control of a maximum to 300 °C.

2.3. Procedure

TG-FTIR experiments were performed using the abovementioned TGA/DSC1 thermogravimetric analyzer system coupled with the said Nicolet iS10 FTIR spectrometer. In this work, during the tests, approximately 20 mg of each sample was heated in the TG at three heating rates (10, 20, and 50 °C/min) in

the temperature range of 50–850 °C under N_2 environment (supplied at a constant rate of 50 ml·min^{-1} under normal conditions) as the purge gas. The heating times of oil shale samples at three heating rates were 80 min (10 °C/min), 40 min (20 °C/min) and 16 min (50 °C/min), and were kept at 850 °C for 7 min. Blank correction runs were carried out to minimize the buoyancy effect. The stainless steel pipe and gas cell (20 cm optical path length) were heated at 150 °C to minimize secondary reactions and tar condensation. The mass loss of each sample was recorded and the changes of the gaseous products amounts with rising temperatures were monitored via FTIR spectrometry. Experiments were repeated at least twice to ensure their reproducibility as well as accuracy of data. According to the reported FTIR absorption characteristic bands of different substances [21, 22], the quantitative analysis of pyrolysis products CH_4, CO, CO_2, H_2O and shale oil was made using the pertinent method for the evolved multi-component gaseous mixtures combined with TG-FTIR [23, 24], and the OMNIC (Thermo Electron, America) software.

2.4. Experimental results and discussion

2.4.1. TGA analysis of the thermal degradation of oil shale

Pyrolysis thermogravimetric (TG) and differential thermogravimetric (DTG) plots for oil shale are depicted in Figure 1.

It is evident from the TG and DTG curves in Figure 1 that the pyrolysis process of Huadian oil shale takes place in three distinct phases: 1) the drying phase (50–200 °C), 2) the organic matter decomposition phase (200–600 °C), and 3) the inorganic matter decomposition phase (600–750 °C). Weight loss in the drying phase is primarily attributed to moisture loss, which includes the loss of absorbed and interlayer water from clay minerals. Meanwhile, the softening and molecular rearrangement, associated with the release of gases from kerogen prior to its decomposition to bitumen, may occur in addition to water moisture loss [25]. Weight loss in the drying phase

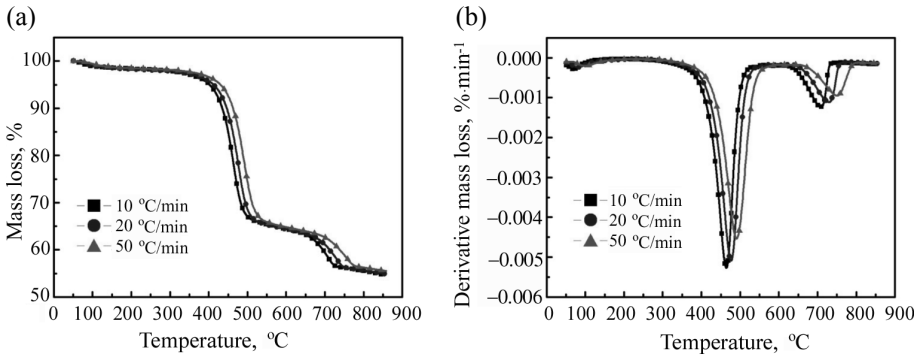

Fig. 1. Non-isothermal TG (a) and DTG (b) curves of oil shale at various heating rates.

in the temperature range of 200–600 °C is predominantly the result of the thermal decomposition of hydrocarbonaceous material. In this phase, weight loss at temperatures up to 400 °C is negligible and the corresponding curves exhibit a zero slope. However, when the temperature has reached 400 °C, the decomposition of shale dramatically intensifies up to 600 °C. As the DTG plot in Figure 1 illustrates, an evident peak appears during the drying phase, which is indicative of the evaporation of hydrocarbons. Involving the decomposition of organic matter including bitumen and kerogen, the second phase of pyrolysis (200–600°C) is considered to be the main thermal decomposition stage in the production of shale oil [26]. During the third, inorganic matter decomposition phase of oil shale pyrolysis (600–750 °C), the mass loss is governed by the thermal decomposition of inorganic minerals, such as carbonates and clay minerals, forming new peaks on the DTG curve. During the pyrolysis process of oil shale, at low temperatures the macromolecules in oil shale break to release low molecular weight volatiles in the form of gaseous substances and also generate some amount of char intermediates. With rising temperature, the unstable intermediates produced at lower temperatures will be further polymerized into more stable intermediates accompanied by the release of volatiles; these volatiles are eventually converted into char by several closely related mechanisms, which include the dehydrogenation of highly olefinic radicals and the condensation/polymerization/dehydrogenation of heavy aromatic radicals [27, 28].

Figure 1 shows the temperatures of maximum degradation rate and weight loss at different heating rates. The weight loss of the sample is indicative of the extent of the pyrolysis reaction which is found to decrease as the heating rate increases from 10 to 50 $°C \cdot min^{-1}$. It can also be observed that the maximum rate of decomposition increases as the heating rate increases, which may be attributed to the heat flux and initiation of secondary cracking reactions. At lower temperatures, oil shale particles will have a sufficient amount of time to be uniformly heated, allowing slow reactions to take place. However, with high heating rates there is not enough time for the sample to be uniformly heated, which would allow the initiation of multiple complex parallel and series reactions of hydrocarbon evolution [26].

2.4.2. Evolved gas analysis by FTIR

Figure 2 illustrates the evolution rate curves of Huadian oil shale pyrolysis products CH_4, CO, CO_2, H_2O and shale oil at various heating rates (10, 20 and 50 °C/min). As a typical example, when the heating rate was 20 $°C \cdot min^{-1}$, below 350 °C a small amount of CO_2 (a characteristic absorption band at 2358 cm^{-1}) began to release from the sample. In oil shale pyrolysis, the emission of CO_2 at low temperatures is primarily ascribed to the decarboxylation/decarbonylation reactions of carboxylic and carbonyl groups attached to aromatic and aliphatic structures. The CO_2 profile reveals two prominent emission peaks at 465 and 725 °C. The quicker release of

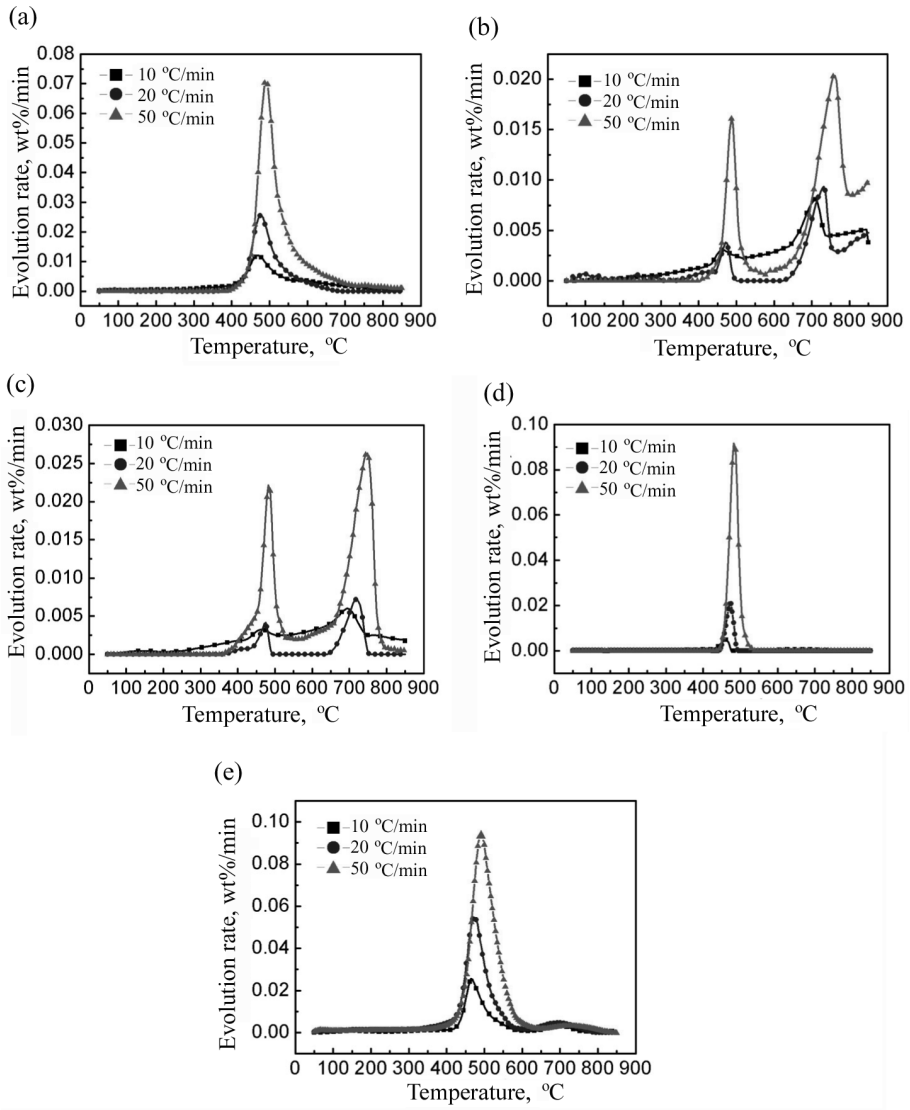

Fig. 2. Evolution rate plots of Huadian oil shale pyrolysis products at various heating rates: (a) CH_4; (b) CO; (c) CO_2; (d) H_2O; (e) shale oil.

CO_2 at high temperatures is attributed to the decomposition of carbonates. The CO (a characteristic absorption band at 2182 cm^{-1}) evolution pattern demonstrates the first evolution peak at about 455 °C and as the temperature increases, the emission of CO continuously increases and reaches maximum at 725 °C due to the reducing reaction of CO_2 and char at high temperatures. CH_4 (a characteristic absorption band at 3017 cm^{-1}) and shale oil began to release at about 400 °C. The release of CH_4 occurred during a wide temperature range (385–675 °C) with a peak of emission centered at 465 °C.

The H_2O (a characteristic absorption band at 3795 cm^{-1}) emission profile during the Huadian oil shale pyrolysis displays evolution peaks at 455 °C that can be assigned to condensation reactions [26, 29]. The temperature of the maximum evolution rate of the pyrolysis product shifted toward higher temperatures with an increase in heating rate. These results are also consistent with thermogravimetric measurements. The key parameters of Huadian oil shale pyrolysis products are shown in Table 2. These parameters include product yields and characteristic temperatures such as the starting (T_{onset}) and final (T_{final}) temperature of each degradation step as well as the maximum release temperature (T_{max}) of Huadian oil shale pyrolysis products at the heating rates tested.

Oil shale devolatilization is a process that transforms oil shale at elevated temperatures, yielding gases, shale oil and char. Shale oil is defined as the room-temperature condensible formed during oil shale devolatilization. Gas formation can often be related to the thermal decomposition of specific functional groups in oil shale. The release of CH_4 is primarily attributed to the break of C–H functional groups from aliphatic compounds, release of CO_2 from the cracking and reformation of carbonyl and carboxyl groups of organics, release of CO from the breaking of C–O–C and C=O functional groups, and release of H_2O from the breaking of O–H functional groups [26]. So far the literature has reported the preliminary study of the chemical structure of oil shale via constructing a carbon skeleton model. It is an intuitive research strategy to draw lessons from the results of research of coal chemical structure and pyrolysis mechanism to apply them for similar oil shale studies. It is generally agreed upon amongst research groups that coal consists mainly of condensed aromatic nuclei cross-linked with ether, methylene, or other bridges/functional groups in peripheral positions.

Table 2. The key parameters of Huadian oil shale pyrolysis products

Product	Heating rate, °C · min^{-1}	T_{onset}, °C	T_{max}, °C	T_{final}, °C	Yield, %
CH_4	10	382	455	672	0.45018
	20	385	465	675	0.45004
	50	387	482	680	0.44973
CO	10	300	448.700	850	0.187
	20	350	455.725	850	0.18707
	50	400	481.748	850	0.18691
CO_2	10	250	455.690	850	0.96404
	20	350	465.725	752	0.94831
	50	352	468.743	790	0.96384
H_2O	10	397	450	475	4.4894
	20	400	455	492	4.48456
	50	403	458	530	4.48408
Shale oil	10	332	452	600	17.65628
	20	335	465	616	17.61571
	50	340	491	630	17.5782

The aromatic nuclei in low rank coal primarily consist of benzene and naphthalene rings, whereas in bituminous coal they are composed of phenanthrene, anthracene and pyrene rings. Solomon et al. [8–10, 30] have established that the pyrolysis process of coal is the combination of the following steps: 1) disruption of hydrogen bonds, 2) vaporization and transport of non-covalently bonded "guest" molecules (molecular phase), 3) low temperature crosslinking (in low rank coals), 4) bridge breaking to fragment the macromolecular network, 5) hydrogen utilization to stabilize free radicals, 6) vaporization and gas phase transport of light fragments, 7) moderate temperature crosslinking to resolidify the macromolecular network, 8) decomposition of functional groups to produce lightweight species, and 9) high temperature condensation of the macromolecular network via hydrogen elimination.

3. FG-DVC model for oil shale pyrolysis

The FG-DVC model of coal pyrolysis describes the evolution of tar, carbon, hydrogen, and oxygen gas species. It combines the functional group (FG) model for gas evolution and the statistical depolymerization, vaporization and crosslinking (DVC) model for tar formation. The composition and kinetic parameters as input parameters of the FG-DVC model are obtained by the TG-FTIR experiment. Tables 1 and 2 present the input parameters of the FG-DVC model (20 °C·min^{-1} as a typical example). The method to calculate the kinetic parameters and predict volatile yields by employing the FG-DVC model is described in the next section.

3.1. The calculation of kinetic parameters

The kinetic parameters of gas evolution during oil shale pyrolysis were obtained by the method previously reported in the literature [31–33].

The experiments employ a linear heating rate (dT/dt = constant). In the case of a simple first order reaction, such as B→C, the rate of product evolution is:

$$\frac{dC}{dT} = \left(\frac{AC_0}{H}\right)\exp\left[-\frac{E}{RT} - \frac{A}{H}\int_0^T \exp\left(\frac{-E}{RT}\right)dT\right], \tag{1}$$

where T is the temperature, H is the heating rate, E and A represent the activation energy and Arrhenius pre-exponential factor, respectively, and R is the gas constant.

Equation (3) is typically simplified using the approximation:

$$\int_0^T \exp\left(\frac{-E}{RT}\right)dT = \left(\frac{RT^2}{E}\right)\exp\left(\frac{-E}{RT}\right). \tag{2}$$

Substitution of Equation (2) into Equation (1) yields:

$$\frac{dC}{dT} = \frac{AC_0}{H} \exp\left[-\frac{E}{RT} - \frac{ART^2}{HE} \exp\left(-\frac{E}{RT} \right) \right]. \tag{3}$$

The above approach is utilized to obtain the necessary kinetic parameters of gas evolution during Huadian oil shale pyrolysis, as shown in Table 3.

Table 3. The kinetic parameters of gas evolution during Huadian oil shale pyrolysis

Product	Heating rate, $°C \cdot min^{-1}$	E, $kJ \cdot mol^{-1}$	A, s^{-1}	Functional group source	R^2
CH_4	10	183	3.3×10^9	R–O–CH_3 R–CH_3	0.965
	20	191	3.3×10^9		0.984
	50	204	3.3×10^9		0.991
CO	10	221	2.8×10^{13}	R–O–R	0.946
	20	205	2.8×10^{13}		0.952
	50	233	2.8×10^{13}		0.971
CO_2	10	242	2.4×10^{10}	R–COOH	0.969
	20	221	2.4×10^{10}		0.968
	50	267	2.4×10^{10}		0.981
H_2O	10	209	2.8×10^{13}	R–OH	0.933
	20	220	2.8×10^{13}		0.936
	50	233	2.8×10^{13}		0.940
Shale oil	10	217	2.8×10^{13}	Macromolecular network	0.949
	20	236	2.8×10^{13}		0.972
	50	261	2.8×10^{13}		0.988

3.2. The prediction of volatile yields by using the FG-DVC model

The FG-DVC model [8–10, 30, 34] suggests that the "evaporation" of a component to the gas phase is depicted by diminishing the Y_i dimension from its initial value, Y_0, to the final value, zero. Thus, the decrease in Y_i is a first-order process:

$$\frac{dY_i}{dt} = -k_i Y_i, \tag{4}$$

$$Y_i = Y_i^0 e^{-k_i t}, \tag{5}$$

where k_i is the distributed rate for species i.

The evolution of a component into tar is described by the first-order diminishing of the X dimension from its initial value, X_0, to the final value, zero; thus, the decrease in X is a first-order process:

$$\frac{dX}{dt} = -k_{tar} X. \tag{6}$$

$$X = X^0 e^{-k_{\text{tar}} t}. \tag{7}$$

The fractional amount of a particular functional group component in char is:

$$W_{\text{i}}(\text{char}) = (1 - X^0 + X) Y_{\text{i}}. \tag{8}$$

The evolution of each gas species is assumed to be a first-order reaction:

$$\frac{dW_{\text{i}}(\text{gas})}{dt} = k_{\text{i}} W_{\text{i}}(\text{char}). \tag{9}$$

The tar composition is tracked by summing the contributions of functional groups evolved with tar. The rate of evolution of each group is:

$$\frac{dW_{\text{i}}(\text{tar})}{dt} = -(dX/dt) Y_{\text{i}}. \tag{10}$$

Therefore, the time dependent weight fractions of char, gas and tar are:

$$W_{\text{i}}(\text{tar}) = \int_0^t \left(-\frac{dX}{dt} \right) Y_{\text{i}} dt = (X^0 Y_{\text{i}}^0 - X Y_{\text{i}}) \frac{k_x}{k_{\text{i}} + k_x}. \tag{11}$$

$$W_{\text{i}}(\text{gas}) = \int_0^t k_{\text{i}} (1 - X^0 + X) Y_{\text{i}} dt = (1 - X^0)(Y_{\text{i}}^0 - Y_{\text{i}}) + W_{\text{i}}(\text{tar}) \frac{k_{\text{i}}}{k_x}. \tag{12}$$

The evolution of CH_4, CO, CO_2, H_2O and shale oil can be described by Equation (12). The predicted and measured evolution curves of CH_4, CO, CO_2, H_2O and shale oil of Huadian oil shale at three heating rates (10, 20 and 50 °C/min) are presented in Figure 3.

As illustrated in Figure 3 and comparison with TG-FTIR experimental data shows, the FG-DVC model quite accurately predicts the pyrolysis gases and shale oil yields. This is supportive of that the pyrolysis mechanism of coal suggested by Solomon et al. [8–10] could provide a feasible theoretical basis for the evolution procedure of light gases and shale oil in the pyrolysis process of oil shale. It is beyond doubt that the oil shale pyrolysis is an extremely complex process. In this work, a simplified FG-DVC model was employed to study the process, yet the entirety of it is still not fully understood. The corresponding simplifications on the transportation of tar and the devolatilization process of gas shale via a first-order reaction resulted in the deviation between the predicted model values and experimental data.

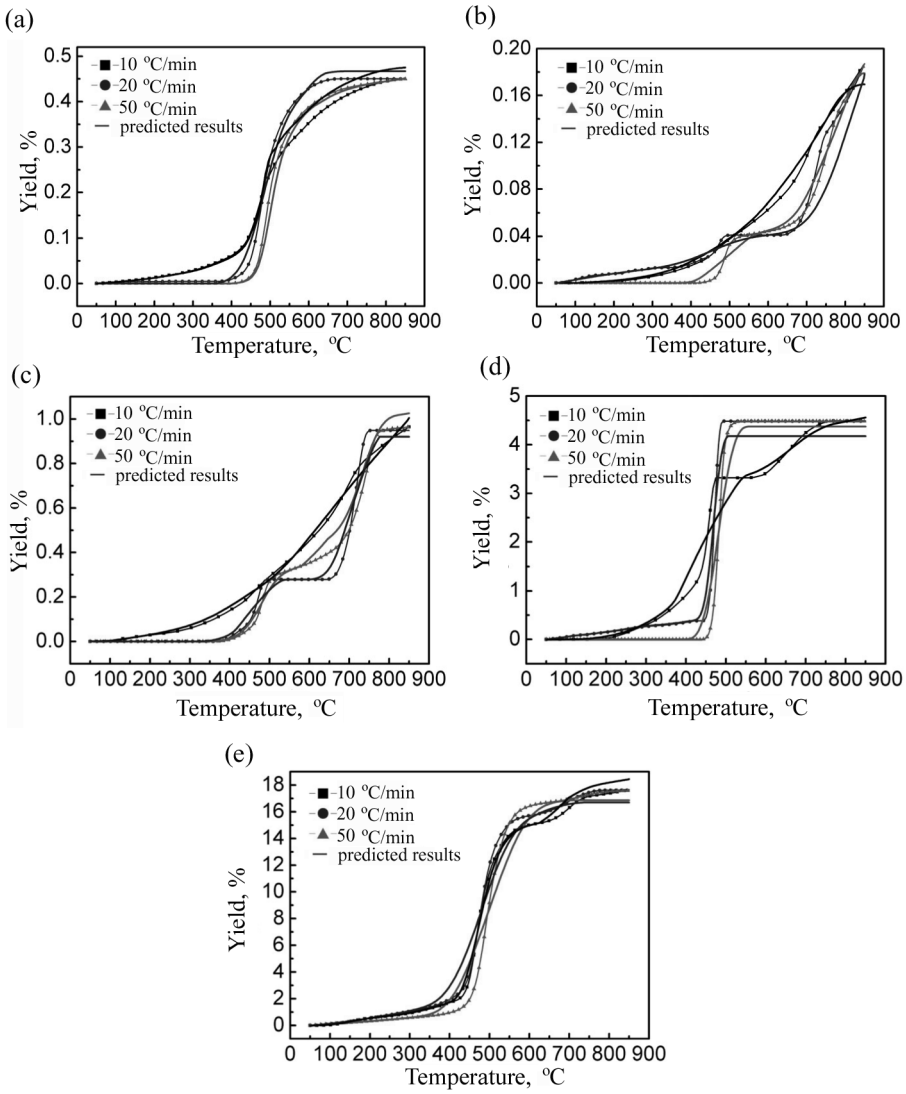

Fig. 3. Evolution curves of Huadian oil shale pyrolysis products at various heating rates: (a) CH_4; (b) CO; (c) CO_2; (d) H_20; (e) shale oil.

4. Conclusions

In this work, TG-FTIR analysis was employed to study the pyrolysis process of Huadian oil shale at three different heating rates. Input parameters of the FG-DVC model were obtained via analysis of the obtained experimental data. Furthermore, predictions were made on the yield of four light gases and shale oil during the pyrolysis process using the FG-DVC model. The following conclusions can be made:

(1) TG-FTIR demonstrated that the pyrolysis process of Huadian oil shale can be divided into three phases. The primary phase occurs between 200 and 600 °C, during which the majority of pyrolysis products completely evolve. The temperature of maximum weight loss rate increases with an increase in the heating rate. The evolution of light gases directly coincides with the decomposition of the precursor functional group.

(2) The values of the activation energy (E) and pre-exponent factor (A) of four light gases and shale oil are between 183 and 270 $kJ \cdot mol^{-1}$ and from 3.3×10^9 to 2.8×10^{13} s^{-1}, respectively, through mathematical analysis of TG-FTIR experimental data.

(3) Comparison of the predicted yield values of pyrolysis products based on the FG-DVC model with experimental data obtained by TG-FTIR at three heating rates was made. The predicted values conformed well to the experimental data with only slight deviations, indicating that the FG-DVC model can provide an effective theoretical basis for revealing the relationship between the chemical structure and pyrolysis products of oil shale.

Acknowledgments

This work was supported by the National Natural Science Foundation of China (No. 51276034) and the Program for Changjiang Scholars and Innovative Research Team in University (IRT13052).

REFERENCES

1. Wang, S., Jiang, X., Han, X., Tong, J. Investigation of Chinese oil shale resources comprehensive utilization performance. *Energy*, 2012, **42**(1), 224–232.
2. Qian Jialin, Yin Liang. *Oil Shale: Petroleum Alternative*. China Petrochemical Press, 2010.
3. Qian, J., Wang, J., Li, S. Oil shale development in China. *Oil Shale*, 2003, **20**(3S), 356–359.
4. Gürüz, G. A, Üçtepe, Ü., Durusoy, T. Mathematical modeling of thermal decomposition of coal. *J. Anal. Appl. Pyrol*., 2004, **71**(2), 537–551.
5. Anthony, D. B., Howard, J. B. Coal devolatilization and hydrogasification. *AIChE J.*, 1976, **22**(4), 625–656.
6. Howard, J. B. Fundamentals of coal pyrolysis and hydropyrolysis. In: *Chemistry of Coal Utilization*, Second Supplementary Volume (Elliott, M. A., ed.). John Wiley & Sons, 1981, 665–784.
7. Campbell, J. H., Gallegos, G, Gregg, M. Gas evolution during oil shale pyrolysis. 2. Kinetic and stoichiometric analysis. *Fuel*, 1980, **59**(10), 727–732.
8. Solomon, P. R., Hamblen, D. G., Carangelo, R. M., Serio, M. A., Deshpande, G. V. General model of coal devolatilization. *Energ. Fuel*., 1988, **2**(4), 405–422.
9. Solomon, P. R., Hamblen, D. G., Yu, Z. Z., Serio, M. A. Network models of coal thermal decomposition. *Fuel*, 1990, **69**(6), 754–763.

10. Solomon, P. R., Hamblen, D. G., Serio, M. A., Yu, Z. Z., Charpenay, S. A characterization method and model for predicting coal conversion behaviour. *Fuel*, 1993, **72**(4), 469–488.
11. Niksa, S., Kerstein, A. R. FLASHCHAIN theory for rapid coal devolatilization kinetics. 1. Formulation. *Energ. Fuel*., 1991, **5**(5), 647–665.
12. Grant, D. M., Pugmire, R. J., Fletcher, T. H., Kerstein, A. R. Chemical model of coal devolatilization using percolation lattice statistics. *Energ. Fuel*., 1989, **3**(2), 175–186.
13. Lü, X., Sun, Y., Lu, T., Bai, F., Viljanen, M. An efficient and general analytical approach to modelling pyrolysis kinetics of oil shale. *Fuel*, 2014, **135**, 182–187.
14. Li, S., Yue, C. Study of different kinetic models for oil shale pyrolysis. *Fuel Process. Technol.*, 2004, **85**(1), 51–61.
15. Janković, B. The kinetic modeling of the non-isothermal pyrolysis of Brazilian oil shale: Application of the Weibull probability mixture model. *J. Petrol. Sci. Eng*., 2013, **111**, 25–36.
16. Sun, Y., Bai, F., Lü, X., Jia, C., Wang, Q., Guo, M., Li, Q., Guo, W. Kinetic study of Huadian oil shale combustion using a multi-stage parallel reaction model. *Energy*, 2015, **82**, 705–713.
17. Jones, J. M., Pourkashanian, M., Williams, A., Hainsworth, D. A comprehensive biomass combustion model. *Renew. Ener*., 2000, **19**(1–2), 229–234.
18. De Jong, W., Di Nola, G., Venneker, B. C. H., Spliethoff, H., Wójtowicz, M. A. TG-FTIR pyrolysis of coal and secondary biomass fuels: Determination of pyrolysis kinetic parameters for main species and NO_x precursors. *Fuel*, 2007, **86**(15), 2367–2376.
19. Wang, H., Jiang, X., Yuan, D., Wan, P. Pyrolysis of coal water slurry volatile matter by using FG-DVC model. *CIESC Journal*, 2006, **57**(10), 2428–2432 (in Chinese, summary in English).
20. Wang, Q., Wang, R., Jia, C. X., Ren, L. G., Wang, H. T., Yan, Y. H. FG-DVC model for oil shale pyrolysis. *CIESC Journal*, 2014, **65**(6), 2308–2315 (in Chinese, summary in English).
21. Xu, T., Huang, X. Study on combustion mechanism of asphalt binder by using TG–FTIR technique. *Fuel*, 2010, **89**(9), 2185–2190.
22. Smith, A. L. *Applied Infrared Spectroscopy: Fundamentals, Techniques, and Analytical Problem-Solving*. Wiley, New York, 1979.
23. Chen, L. G., Tun, H. C., Cen, G. F. Quantitative research of evolved gas rate by TGA-FTIR. *Journal of Zhejiang University (Engineering Science)*, 2009, **43**(7), 1332–1336 (in Chinese, summary in English).
24. Chen, L. G., Wu, X. C., Zhou, H., Cen, K. F. Quantitative analysis of multi-component gases mixture evolved in combined TG-FTIR. *Journal of Zhejiang University (Engineering Science)*, 2010, **44**(8), 1579–1583 (in Chinese, summary in English).
25. Jaber, J. O., Probert, S. D. Pyrolysis and gasification kinetics of Jordanian oil-shales. *Appl. Energ*., 1999, **63**(4), 269–286.
26. Al-Harahsheh, M., Al-Ayed, O., Robinson, J., Kingman, S., Al-Harahsheh, A., Tarawneh, K., Saeid, A., Barranco, R. Effect of demineralization and heating rate on the pyrolysis kinetics of Jordanian oil shales. *Fuel Process. Technol*., 2011, **92**(9), 1805–1811.
27. Ballice, L. Effect of demineralization on yield and composition of the volatile products evolved from temperature-programmed pyrolysis of Beypazari (Turkey) oil shale. *Fuel Process. Technol*., 2005, **86**(6), 673–690.

28. Yan, J., Jiang, X., Han, X., Liu, J. A TG–FTIR investigation to the catalytic effect of mineral matrix in oil shale on the pyrolysis and combustion of kerogen. *Fuel*, 2013, **104**, 307–317.
29. Scaccia, S. TG–FTIR and kinetics of devolatilization of Sulcis coal. *J. Anal. Appl. Pyrol*., 2013, **104**, 95–102.
30. Solomon, P. R., Serio, M. A., Suuberg, E. M. Coal pyrolysis: Experiments, kinetic rates and mechanisms. *Prog. Energ. Combust*., 1992, **18**(2), 133–220.
31. Campbell, J. H., Gallegos, G., Gregg, M. Gas evolution during oil shale pyrolysis. 2. Kinetic and stoichiometric analysis. *Fuel*, 1980, **59**(10), 727–732.
32. Huss, E. B., Burnham, A. K. Gas evolution during pyrolysis of various Colorado oil shales. *Fuel*, 1982, **61**(12), 1188–1196.
33. Suuberg, E. M., Sherman, J, Lilly, W. D. Product evolution during rapid pyrolysis of Green River Formation oil shale. *Fuel*, 1987, **66**(9), 1176–1184.
34. Solomon, P. R., Colket, M. B. Coal devolatilization. *Symposium (International) on Combustion*, 1979, **17**(1), 131–143.

Presented by J. Qian
Received May 9, 2015